Journal of Molecular and Cellular Cardiology 129 (2019) 303–313

Contents lists available at ScienceDirect

Journal of Molecular and Cellular Cardiology

journal homepage: www.elsevier.com/locate/yjmcc

Original article

In vitro analysis of arrhythmogenic cardiomyopathy associated desmoglein-2 (*DSG2*) mutations reveals diverse glycosylation patterns

Jana Davina Debus[a], Hendrik Milting[a,*], Andreas Brodehl[a], Astrid Kassner[a], Dario Anselmetti[b], Jan Gummert[c], Anna Gaertner-Rommel[a]

[a] *Erich and Hanna Klessmann Institute for Cardiovascular Research and Development, Heart and Diabetes Center NRW, University Hospital of the Ruhr-University Bochum, Bad Oeynhausen, Germany*
[b] *Faculty of Physics, Experimental Biophysics and Applied Nanoscience, Bielefeld Institute for Nanoscience (BINAS), Bielefeld University, Bielefeld, Germany*
[c] *Clinic for Thoracic and Cardiovascular Surgery, Heart and Diabetes Center NRW, University Hospital of the Ruhr-University Bochum, Bad Oeynhausen, Germany*

ARTICLE INFO

Keywords:
Desmoglein-2
N-glycosylation
Arrhythmogenic right ventricular cardiomyopathy
Desmosomes
Cardiovascular genetics

ABSTRACT

Arrhythmogenic right ventricular cardiomyopathy is a heritable cardiac disease causing severe ventricular arrhythmias, heart failure and sudden cardiac death. It is mainly caused by mutations in genes encoding several structural proteins of the cardiac desmosomes including the *DSG2* gene encoding the desmosomal cadherin desmoglein-2.

Although the molecular structure of the extracellular domain of desmoglein-2 is known, it remains an open question, how mutations in *DSG2* contribute to the pathogenesis of arrhythmogenic right ventricular cardiomyopathy. In the present study, we analyzed the impact of different *DSG2* mutations on the glycosylation pattern using de-glycosylation assays, lectin blot analysis and genetic inhibition studies. Remarkably, wildtype and mutant desmoglein-2 displayed different glycosylation patterns, although the investigated *DSG2* mutations do not directly affect the consensus sequences of the N-glycosylation sites.

Our study reveals complex molecular interactions between *DSG2* mutations and N-glycosylations of desmoglein-2, which may contribute to the molecular understanding of the patho-mechanisms associated with arrhythmogenic right ventricular cardiomyopathy.

1. Introduction

Arrhythmogenic right ventricular cardiomyopathy (ARVC) is a heritable cardiac disease associated with ventricular arrhythmias, heart failure and sudden cardiac death especially in young athletes [1,2]. ARVC is pathologically characterized by a progressive loss of cardiomyocytes and fibro-fatty tissue replacement predominantly in the right ventricle [3,4]. About 50% of the ARVC patients present one or more mutations in genes encoding structural proteins especially of the cardiac desmosomes [5–10] including mutations in *DSG2,* encoding desmoglein-2 (DSG2) [11–13]. Desmosomes are adhesive cell-cell junctions that anchor the intermediate filament system to the plasma membrane in adjacent cells contributing to the nano-mechanical integrity of the myocardium and the epidermis [14].

DSG2 and desmocollin-2 (DSC2) are members of the cadherin family and connect neighboring cardiomyocytes *via* interaction of their extracellular domains [15,16]. The homo- and heterophilic protein-protein interactions between the desmosomal cadherins are Ca^{2+} dependent [17,18]. However, the molecular patho-mechanisms of *DSG2* mutations contributing to the pathogenesis of ARVC are widely unknown. Harrison et al. 2016 determined the molecular structure of the extracellular DSG2 domains revealing five N-glycosylation sites at N112, N182, N309, N462 and N514 and three O-mannosylation sites at T480, T482 and T484 [16]. However, to the best of our knowledge the impact of ARVC associated *DSG2* mutations on the glycosylation pattern has not been investigated before. Therefore, four different genetic *DSG2* mutations localized within each extracellular cadherin domain (ECD) were selected to investigate their putative influence on glycosylation.

In the present study, we analyzed the impact of different ARVC associated *DSG2* mutations on the glycosylation patterns using enzymatic and chemical de-glycosylation assays, lectin blot analysis and by genetic engineered glycosylation deficient mutants. Remarkably, wildtype (WT) and mutant DSG2 displayed different glycosylation patterns, although the ARVC associated mutations do not directly affect the consensus sequences of the N-glycosylation sites. Our study reveals a

* Corresponding author.
E-mail address: hmilting@hdz-nrw.de (H. Milting).

https://doi.org/10.1016/j.yjmcc.2019.03.014
Received 18 June 2018; Received in revised form 6 February 2019; Accepted 14 March 2019
Available online 15 March 2019

molecular interplay between ARVC associated *DSG2* mutations and the N-glycosylation state of DSG2, which may contribute to the understanding of the ARVC associated patho-mechanisms.

2. Materials and methods

2.1. Cell culture

Stably transfected HT1080 cells [19] were cultivated in Dulbecco's Modified Eagle Medium (DMEM, 4.5 g/L D-glucose, Thermo Fisher Scientific) supplemented with 10% FCS Gold (PAA), 100 U/mL Penicillin/100 µg/mL Streptomycin and 2,5 µg/mL Amphotericin B (Biochrom) and 600 ng/mL Puromycin (Invivogen) (37 °C, 5% CO_2).

2.2. Differentiation of human induced pluripotent stem cells into cardiomyocytes

Human induced pluripotent stem cells (hiPSC, NP0040-8, UKKi011-A) were kindly provided by Dr. Tomo Saric (University of Cologne, Germany) and were cultured in Essential E8 Medium (Thermo Fisher Scientific) on Vitronectin (#A14700, Thermo Fisher Scientific) coated cell culture dishes. The medium was changed every day. When the hiPSC reached about 85% confluence, the differentiation into cardiomyocytes was initiated. The medium was changed against RPMI1640 (#72400047, Thermo Fisher Scientific) supplemented with human albumin (500 mg/L, Sigma-Aldrich), L-ascorbic acid-2-phosphate (100 mg/L, Sigma-Aldrich) and the GSK3 inhibitor CHIR99021 (4 µM, Sigma-Aldrich) for two days. Afterwards, the medium was changed against RPMI1640 (500 mg/L human albumin; 100 mg/L L-ascorbic acid-2-phosphate) supplemented with IWP2 (5 µM, Sigma-Aldrich). At day 4 and 6 of the differentiation process, the medium was changed against RPMI1640 (500 mg/L human albumin; 100 mg/L L-ascorbic acid-2-phosphate). Starting from day 8 after initiation, the medium was changed every two days against RPMI1640 supplemented with B27 Supplement (#17504044, Thermo Fisher Scientific) and the cells were daily observed for contractility. All media used for the differentiation were supplemented with penicillin/streptomycin.

2.3. Construction of plasmids

The human c-terminally RGS/H_6 tagged DSG2-extracellular cadherin domains 1–4 (DSG2-ECD) of WT and mutants were cloned in pLPCX expression plasmid (Clontech) and the cDNAs of full length WT and mutant DSG2 were generated accordingly from pEYFP-N1 plasmids (Clontech) as described before [19]. The N-glycosylation sites N112, N182, N309, N462 and N514 were mutated to Q using Quick Change Lightning Site-Directed Mutagenesis Kit (Agilent Technologies).

2.4. Purification of recombinant DSG2

WT and mutant DSG2-ECDs were stably expressed in HT1080 cells as previously reported [19]. Recombinant DSG2-ECDs were purified from cell culture supernatants by immobilized metal affinity chromatography (IMAC) on HisTrap excel columns (GE Healthcare) according to the manufacturer's instructions. The protein solutions were concentrated with Amicon Ultra-15 Centrifugal Filter Units (30,000 MWCO, Millipore) and dialyzed against 10 mM HEPES, 150 mM NaCl, pH 7.4. Purified DSG2-ECDs were analyzed by sodium dodecyl sulfate polyacrylamide gel electrophoresis (SDS-PAGE) in combination with Coomassie brilliant blue staining or Western blot analysis.

2.5. Peptide N-glycosidase F (PNGase F) digest

Purified DSG2-ECDs were treated with PNGase F (New England Biolabs) according to the manufacturer's protocol under denaturing conditions at 37 °C for 20 h. Proteins were analyzed before and after enzymatic deglycosylation using SDS-PAGE and Coomassie brilliant blue staining.

2.6. Sugar staining with Pro-Q® Emerald 300 glycoprotein gel and blot stain

For glycoprotein detection in gels the Pro-Q® Emerald 300 Glycoprotein Gel and blot stain kit (Thermo Fisher Scientific) was used according to the manufacturer's instructions. Purified DSG2-ECDs were analyzed before and after enzymatic deglycosylation with PNGase F using SDS-PAGE and subsequent Pro-Q® Emerald 300 Glycoprotein Gel and blot stain.

2.7. Lectin blotting

Lectin blot analyses were performed to determine carbohydrate moieties using DIG Glycan Differentiation Kit (Roche). Purified DSG2-ECDs were analyzed before and after enzymatic deglycosylation with PNGase F using SDS-PAGE and Western blotting. After treatment with blocking reagent, the membranes were incubated with digoxigenin labeled lectins according to the manufacturer's instructions.

2.8. Transfection of HT1080 cells

Lipofectamine LTX (Thermo Fisher Scientific) was used according to the manufacturer's protocol for cell transfections. Transfected cells were selected with 600 ng/mL puromycin (Invivogen).

2.9. Transfection of hiPSC derived cardiomyocytes

HiPSC were transfected according to the Amaxa® 4D-Nucleofector® Basic Protocol for Human Stem Cells. Briefly 2×10^5 cells were transfected with 400 ng plasmid DNA using the P3 Primary Cell 4D-Nucleofector® X Kit. For electroporation with the 4D-Nucleofector™ (Lonza) program CA-137 was used. After electroporation cells were incubated at 37 °C for 10 min and seeded on fibronectin-coated Nunc™ Lab-Tek Permanox Chamber Slides. After 48 h transfected cells were fixed with 4% (w/v) PFA/PBS-solution, permeabilized with 0.25% Triton X-100 solution, blocked with 1% (w/v) BSA in PBS and incubated with a mouse anti α-actinin antibody as cardiomyocyte marker (1:100; A7732, Sigma-Aldrich) over night. As a secondary antibody a Cy3-labeled goat anti mouse antibody (1:100; 115-165-068 Jackson ImmunoResearch) was used. Fixed cells were additionally labeled with DAPI. As mounting medium Mowiol 4-88 was used.

2.10. Detection of secreted DSG2-ECD N-glycosylation mutants

1×10^6 stably transfected cells were seeded in six well plates and cultured in serum-containing media for 24 h. The cells were washed twice with phosphate buffered saline (PBS, Thermo Fisher Scientific). Afterwards, the cells were cultured in DMEM without serum for 48 h and the supernatants were collected, centrifuged at 21,000 ×g for 10 min and analyzed by SDS-PAGE.

2.11. Tunicamycin treatment

1×10^6 stably transfected cells were cultured in six well plates in DMEM supplemented with FCS and tunicamycin (10 µg/mL; solved in dimethyl sulfoxide, DMSO; Sigma-Aldrich) for 24 h. As a negative control, cells were treated with the corresponding amount of DMSO. The cells were washed twice with PBS and were cultured for additional 24 h in DMEM without serum containing 10 µg/mL tunicamycin or DMSO. Afterwards the supernatants were collected, centrifuged at 21,000 ×g for 10 min and analyzed by SDS-PAGE.

2.12. Immunoblotting

Purified recombinant DSG2-ECD or cell culture supernatants were denatured in SDS sample buffer at 95 °C for 5 min and separated by SDS-PAGE. Afterwards, the proteins were transferred to nitrocellulose membranes as previously described [19]. After blocking with 5% skimmed milk in Tris buffered saline (TBS) containing 0.05% Tween 20 (TTBS), the membranes were incubated with anti-DSG2 antibodies (Acris, BM5016), anti-H_6-tag antibodies (Abcam, ab18184) (1:1000) or anti-ubiquitinated protein antibodies (Abcam, ab137025) in TTBS over night at 4 °C. The membranes were washed three times with TTBS and were incubated with horseradish peroxidase (HRP)-conjugated anti-mouse immunoglobuline antibodies (BD Pharmingen, 554,002, 1:1000) or HRP-conjugated anti-rabbit antibodies (GE-Healthcare, NA934) for 1 h at room temperature. After the membranes were washed with TTBS and were incubated with WesternBright Quantum HRP substrate (Advansta), the luminescence signals of the proteins bands were documented with a charge coupled device system (Alpha-Innotec).

2.13. Confocal microscopy

Cells were culture and transfected in Lab-Tek II chambers (Thermo Fischer Scientific). 48 h after transfection the cells were analyzed using the TCS SP8 confocal microscope (Leica). EYFP was excited at 488 nm and the emission was detected in the range between 510 and 563 nm.

2.14. Dispase based dissociation assay

Cell–cell adhesion was investigated using a dispase based cell dissociation assay. Stably transfected full-length-*DSG2* WT and mutant-pEYFP/DSC2b-pLPCX HT1080 cells were seeded in 12-well plates and grown to confluence in the presence of 2 mM $CaCl_2$. After two washes with phosphate-buffered saline, the adherent cells were incubated at 37 °C for 20 min with 0.3 mL dispase II (2.4 U/mL, Sigma Aldrich) resulting in a non-adherent cell monolayer. Released monolayers were rotated on an orbital shaker (150 rpm) for 20 min. Finally, cell dissociation was calculated by counting monolayer fragments. Every experimental condition was performed in quadruplicate and repeated five times.

2.15. Molecular modeling

For molecular modeling PyMOL 2.1.1 (Schrodinger, LCC) was used and the mutant amino acid was selected using the mutagenesis tool of the software. For all mutants the rotamer with the highest frequency of occurrence in proteins was chosen. The structure was cleaned within 5A. The polar contacts to other atoms in the object were calculated for wild type and mutant proteins, respectively.

2.16. Statistical analyses

Statistical analyses have been performed with one-way ANOVA with Dunnett's posttest using Prism v5.01 (GraphPad Software). All indicated values are presented as means ± standard derivation (SD).

3. Results

3.1. The recombinantly expressed DSG2-ECD of WT and ARVC associated mutants are differentially modified

Four previously described ARVC associated DSG2 mutations (p.D154E [11], p.D187G [20], p.K294E [13] and p.V392I [11]) located within each ECD were selected to investigate their influence on the glycosylation pattern (Fig. 1). The pathogenetic potential of the DSG2 mutations was classified according to ACMG criteria. The DSG2 mutations p.D154E, p.D187G and p.K294E were classified as variants with uncertain significance whereas DSG2 p.V392I was categorized as likely benign (Table S1, Supplements). Molecular modeling using PyMOL (Fig. 1B) revealed that polar contacts to two calcium ions were abolished by the mutations DSG2 p.D154E and p.D187G, respectively. Polar interaction with T329 was reversed by the mutation DSG2 p.K294E. There were no polar contacts for valine at position 392 according to PyMOL modeling. Therefore, there was no evidence that the mutation p.V392I leads to changes in the molecular structure.

The recombinant ECD of WT and mutant DSG2 were purified by IMAC. Although the mutants differ from DSG2-ECD WT protein by only one amino acid, DSG2-ECD p.D154E and p.K294E displayed a significantly different apparent molecular mass in the SDS-PAGE (Fig. 2A). In contrast to DSG2-ECD WT (apparent molecular mass of 66 kDa) the two mutants DSG2-ECD p.D154E and p.K294E had significantly larger apparent molecular masses of 69 and 70 kDa, respectively (Fig. 2A). These data suggest that the mutants and WT DSG2-ECDs are differentially modified.

3.2. The mutant DSG2-ECD p.D154E is differently N-glycosylated

Recently, the determination of the molecular structure of the extracellular DSG2 domains revealed five N-glycosylation sites [16]. *In silico* prediction tools were used to calculate the N-glycosylation of DSG2-ECD WT and mutants (NetNGlyc 1.0 Server; http://www.cbs.dtu.dk/services/NetNGlyc/). Although the score between WT and mutant DSG2-ECDs differed for some N-glycosylation sites, the *in silico* analysis indicates that WT and mutant DSG2-ECDs are probably glycosylated at the same N-residues (Table S2, Supplements).

We used tunicamycin to inhibit the N-glycosylation of DSG2. These experiments revealed a significantly reduced molecular mass of WT and mutant DSG2-ECD after treatment with tunicamycin (Fig. 2B). Enzymatic N-deglycosylation by PNGase F demonstrated comparable effects (Fig. 2C/D). After treatment with PNGase F, which removes N-linked oligosaccharids from glycoproteins, the apparent molecular masses of DSG2-ECD WT and the mutants p.D154E, p.D187G and p.V392I were not significantly different (≈54 kDa) (Fig. 2C/D). Of note, DSG2-ECD p.K294E had a significantly different molecular mass of 58 kDa (Fig. 2C/D).

N-deglycosylation with PNGase F in combination with Pro-Q® Emerald 300 glycoprotein staining resulted in a loss of fluorescence signal (Fig. 2E), demonstrating the absence of carbohydrates. This suggests that O-mannosylation might not be present in DSG2-ECD WT and mutants or was below the detection limits, respectively.

In summary, our data consistently showed that the mutant DSG2-ECD p.D154E was differentially N-glycosylated in comparison to the WT. The mutant DSG2-ECD p.K294E was not differentially N-glycosylated, as this mutant exhibited no detectable carbohydrate groups after cleavage with PNGase F in combination with Pro-Q® Emerald 300 glycoprotein staining, but still displayed a 4 kDa higher apparent molecular mass in comparison to the other deglycosylated DSG2-ECDs. Thus, the mutant DSG2-ECD p.K294E might be otherwise differently post-translationally modified. Ubiquitination as post-translational modification (PTM) was also excluded for this mutant (Fig. S1, Supplements).

3.3. Mutant DSG2-ECDs p.K294E and p.V392I display differential lectin binding

To determine the sugar moieties of DSG2-ECD WT and mutants, lectin blots were performed. Lectins are carbohydrate-binding proteins from plants recognizing specific sugar moieties [21]. WT and mutant DSG2-ECDs were bound by DSA (*Datura stramonium* agglutinin) and MAA (*Maackia amurensis* agglutinin) indicating the presence of Gal-(1-4) GlcNAc and sialic acid linked (2-3) to galactose in complex N-glycans, respectively (Fig. 3A–B). DSG2-ECD WT and the mutants p.D154E and p.D187G exhibited an interaction with SNA (*Sambuccus nigra*

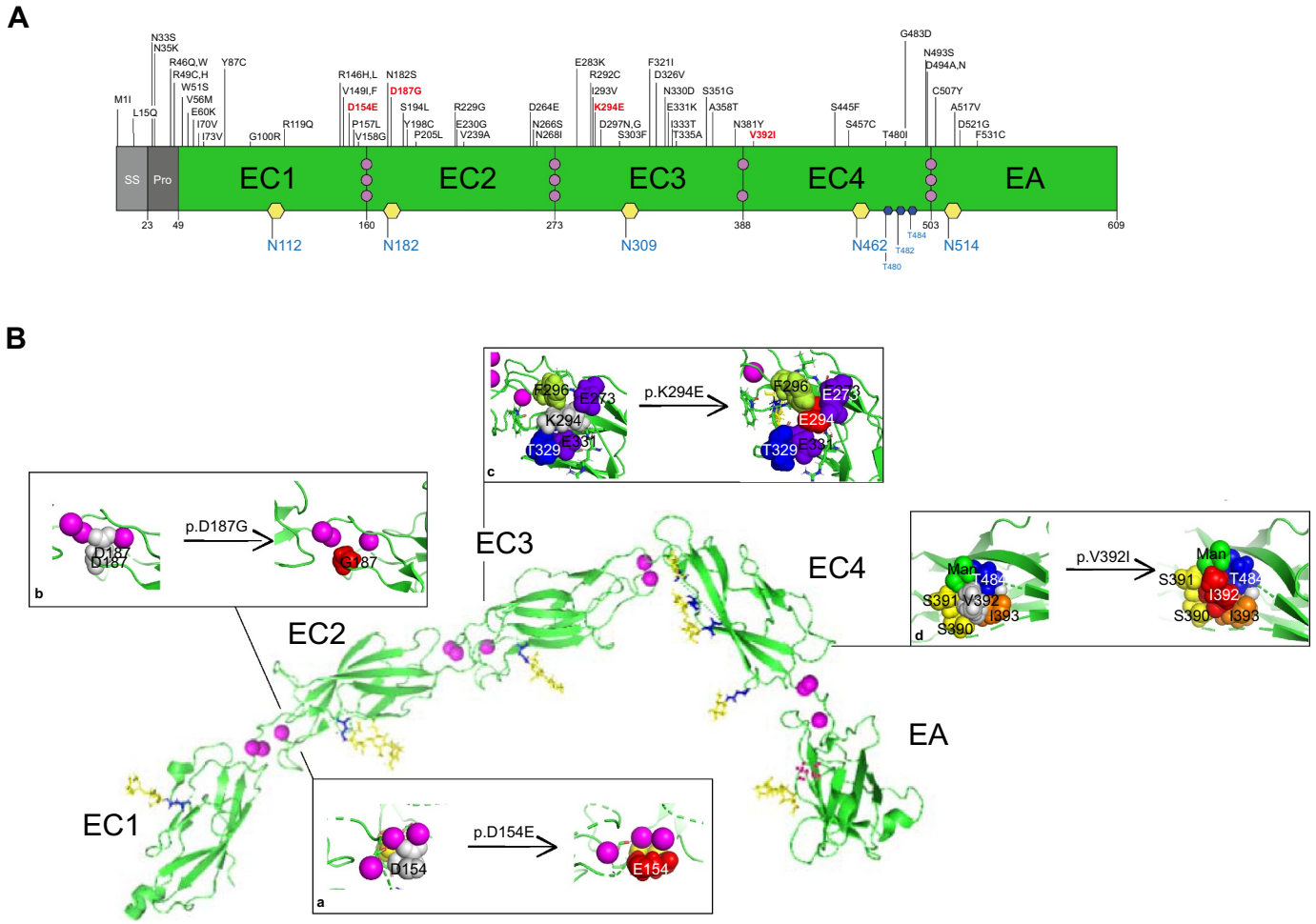

Fig. 1. Molecular structure of the extracellular domains of DSG2.
(A) Schematic overview on the missense mutations in the extracellular domains of DSG2 associated with cardiomyopathy and registered by May 2018 in the Human Gene Mutation Database (HGMD; www.hgmd.cf.ac.uk) or ARVC Database www.arvcdatabase.info Selected missense mutations are given in red, N-glycosylations in yellow, O-mannosylations in blue and position of Ca^{2+} ions in purple (**SS** = signal sequence; **Pro** = prodomain, **EC1–4** = extracellular cadherin domain 1–4; **EA** = extracellular anchor domain). Protein domain positions are taken from UniProt (www.uniprot.org). (B) Molecular modeling of ARVC associated DSG2 variants. The structure of the extracellular domains of DSG2 (5ERD, https://www.rcsb.org/) has been previously determined by Harrison et al. [16]. The protein backbone is shown in green, the Ca^{2+} ions in purple, the sugar residues in yellow and the amino acids carrying the sugar residues are shown in blue. The influence of DSG2 variants (red) on the molecular structure of the extracellular domains was investigated using PyMOL (version 5.1.1, Schrodinger LLC). Amino acids or ions, which are in close proximity to the amino acids D154 (a), D187 (b), K294 (c) and V392 (d) of DSG2 are shown. For D154 and D187 polar contacts exist to two Ca^{2+}-Ions (magenta), which are abolished by the mutations p.D154E and p.D187G, respectively. Polar interaction with T329 (blue) is reversed by the mutation p.K294E. There are no polar contacts for valine at position 392 according to PyMOL. Therefore, there was no evidence from molecular modeling that the mutation p.V392I leads to changes in the molecular conformation.

agglutinin), which recognizes sialic acid linked (2–6) to galactose, whereas the mutants p.K294E and p.V392I were not bound by SNA (Fig. 3C). GNA (*Galanthus nivalis* agglutinin) binding was not detectable (Fig. 3D), suggesting the absence of highly mannosylated oligosaccharides.

After PNGase F treatment of DSG2-ECD WT and mutants no lectin binding was observed (Fig. S2, Supplements), suggesting that potential O-mannosylated glycans would probably not be further elongated. Our data show that WT and mutant DSG2-ECDs do not contain high mannose N-glycans but carry complex N-glycans with varying terminal sialic acid linkage. Of note, the ARVC associated DSG2 mutations p.K294E and p.V392I cause an altered glycosylation pattern.

3.4. Mutant DSG2-ECD p.D154E is differentially glycosylated at p.N182

To determine if one or more specific N-glycosylation sites are altered in the ARVC associated mutants, we used site-directed mutagenesis to inhibit genetically N-glycosylation at specific positions. Therefore, N-glycosylation consensus sequences were changed by substituting asparagine against glutamine residues (p.N112Q, p.N182Q, p.N309Q, p.N462Q). These constructs were recombinantly expressed and the apparent molecular masses of the proteins were determined by SDS-PAGE in combination with Western blot analysis. Completely glycosylated DSG2-ECD WT, its mutants and a construct deficient for all four N-glycosylations were used as a control.

Each of the N-glycosylation deficient DSG2-ECD WT and mutants with one substitution at p.N112Q, p.N182Q, p.N309Q or p.N462Q showed consistently and significantly decreased apparent molecular masses compared to their completely glycosylated controls. This confirms that N-glycosylation was present at all four positions in DSG2-ECD WT as well as in all ARVC associated mutants (Fig. 4A–E). Interestingly, the constructs without N-glycosylation at p.N462 displayed the lowest molecular masses for WT and mutant DSG2 (Fig. 4A–E), suggesting that the largest N-glycosylation is found at this position.

The N-glycosylation deficient DSG2-ECD mutant p.D154E without N-glycosylation at p.N112, p.N309 or p.N462 (Fig. 4F, H, I, J, L, M)

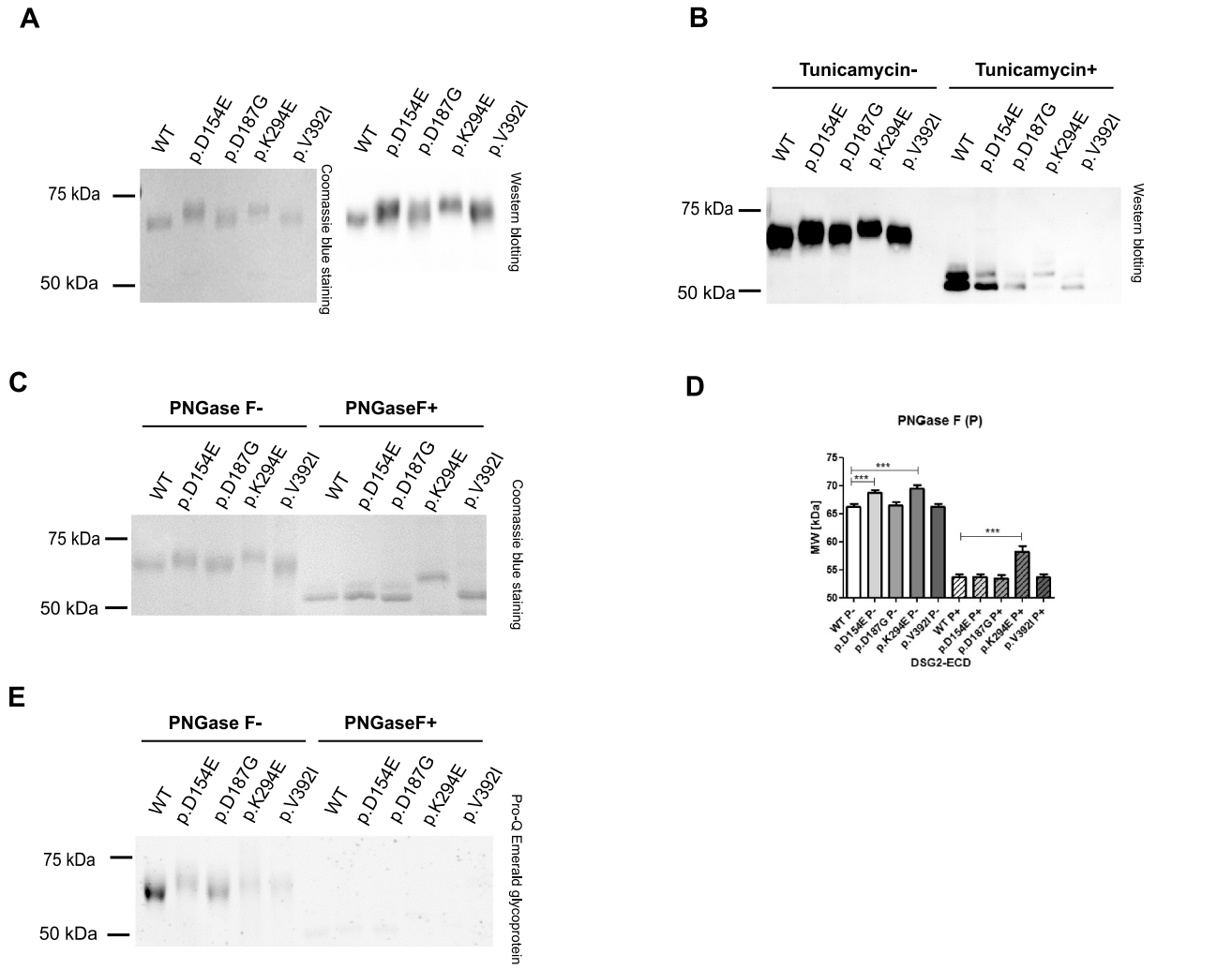

Fig. 2. DSG2-ECD WT and mutants are differently modified.
(A) Coomassie blue staining and Western blot analysis using anti DSG2 antibodies revealed an altered molecular mass of mutant DSG2-ECDs in comparison to the WT. (B) Treatment with N-glycosylation inhibitor tunicamycin in combination with Western blot analysis using anti-H_6-tag antibodies decreased the molecular mass of DSG2-ECD WT and mutants indicating a diverse N-glycosylation of DSG2-ECD p.D154E. (C) Enzymatic N-deglycosylation using PNGase F resulted in a size reduction for DSG2-ECD WT and mutants revealing diverse N-glycosylation of DSG2-ECD p.D154E. (D) Statistical analysis indicates significantly different apparent molecular masses for DSG2-ECD p.D154E and p.K294E. Data are shown as means ± SD. After PNGase F digest DSG2-ECD p.K294E still displays a significantly increased apparent molecular mass suggesting another yet unknown PTM. (E). Treatment with PNGase F in combination with Pro-Q® Emerald 300 glycoprotein staining indicates the complete loss of sugar residues.

displayed significantly larger masses compared to the WT, whereas the mass of the mutant without N-glycosylation at p.N182 was not different from the WT (Fig. 4G, K). This suggests a larger N-glycosylation of the mutation DSG2-ECD p.D154E at p.N182 and may explain the observed differences in SDS-PAGE of the completely-glycosylated proteins. The N-glycosylation deficient DSG2-ECD mutant p.K294E without N-glycosylation at p.N112, p.N182, p.N309 or p.N462 (Fig. 4F–M) always displayed significantly larger masses compared to the WT indicating a further PTM.

3.5. Removal of multiple N-glycosylation sites abolishes the transport of DSG2 to the cell membrane

We used confocal microscopy to investigate if genetic deletion of the N-glycosylation sites is affecting the subcellular distribution of DSG2. We generated mutants missing single N-glycosylation sites and constructs without all N-glycosylation sites. In addition, we constructed mutants with only one remaining N-glycosylation site (Fig. 5A–D). Completely glycosylated DSG2 WT and mutants were found within the HT1080 cells and at the plasma membrane. In contrast, N-glycosylation deficient DSG2 WT and mutants without any N-glycosylation were mainly localized in intracellular structures (Fig. 5A), which are presumably part of the endoplasmic reticulum or the Golgi apparatus, respectively. These findings were consistently found also in hiPSC derived cardiomyocytes (B). Each of the DSG2 WT and mutants without N-glycosylation at p.N112, p.N182, p.N309, p.N462 or p.N514 were found within the cells and at the plasma membrane (Fig. 5C), which was not different from the completely glycosylated proteins. DSG2 mutants lacking all but one N-glycosylation site were still transported to the cell surface (Fig. 5D).

3.6. Cell-cell adhesion strength is affected by DSG2 mutation

To investigate the influence of ARVC associated DSG2 mutations on cell–cell adhesion strength a dispase based cell dissociation assay was performed. The mutant DSG2-ECD p.D187G monolayer could be fragmented into less pieces (8.9 ± 3.8) than the WT (17.5 ± 6.3 [15]) suggesting a stronger cellular interaction. Of note, the number of

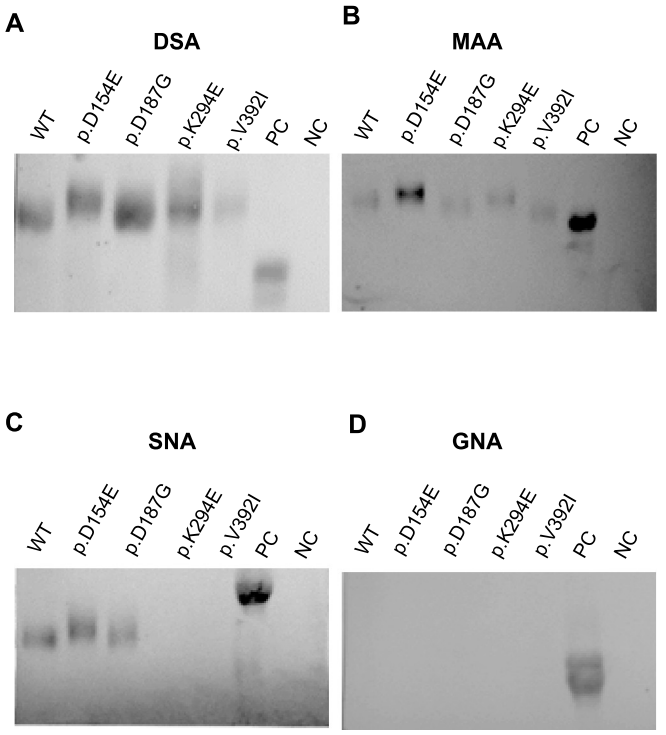

Fig. 3. DIG-labeled lectin blot analysis reveals that DSG2-ECD WT and mutants possess different sugar moieties.
DSG2-ECD WT and mutants show an interaction with DIG-labeled DSA (A) and MAA (B) recognizing Gal1–4GlcNAc in complex N-glycans and sialic acid linked α2–3 to Gal, respectively. WT, p.D154E and p.D187G exhibit an interaction with SNA (C), which recognizes sialic acid linked α2–6 to Gal, whereas p.K294E and p.V392I were not bound by SNA. WT as well as all variants do not interact with GNA (D) recognizing highly mannosylated glycans. As expected, all lectins interact with their appropriate control protein (PC) and do not interact with deglycosylated control protein (NC).

fragments in the dispase assay of the mutant p.K294E (14.8 ± 5.6) was not significantly different from DSG2 WT (Table 1, for a summary of the results see Fig. 6)

4. Discussion

Since the first characterization of ARVC associated *DSG2* mutations in 2006, numerous mutations in *DSG2* and other genes encoding desmosomal proteins have been linked to ARVC [5,9–11]. In public disease databases > 130 different missense, splice site, nonsense or frameshift mutations in *DSG2* are listed (Human Gene Mutation Databank, http://www.hgmd.cf.ac.uk/ac/index.php, [22]; ARVC Database, www.arvcdatabase.info, [23]). However, the pathogenic evidence of the majority of these missense mutations remains unknown, challenging genetic counseling of affected families. Nevertheless different mouse models targeting *Dsg2* suggest the general pathogenic impact of *DSG2* mutations for the development of ARVC: The global *Dsg2* deletion is embryonically lethal in mice [24], whereas the cardiac specific deletion causes cardiomyopathy associated with fibrosis and calcification [25]. Interestingly the deletion of a fragment within the first and second ECDs of murine *Dsg2* causes a similar cardiomyopathy phenotype [26]. Pilichou et al. generated a transgenic mouse overexpressing *Dsg2* p.N271S corresponding to the human *DSG2* p.N266S, which is located within the Ca^{2+}-binding site between EC2-EC3 and resulting in a severe cardiomyopathy [13]. However, the *bi*ventricular phenotype of the murine models does not perfectly fit to the human clinics, since *i.e.* fibro-fatty replacement, which is a hallmark of human ARVC [3,4] is not present. Moreover, the molecular and cellular patho-mechanisms caused by *DSG2* mutations remain also widely unknown in these mouse models.

In clinical setting the vast majority of the mutations in *DSG2*, have to be classified as variants of uncertain significance due to the lack of co-segregation and/or experimental data. Therefore, we decided to analyze these mutations, since they are registered in the ARVC-mutation- and the HGMD-database, which are both frequently used for diagnostic purposes (see also Table S1, Supplements).

Recently, the molecular structure of the complete extracellular domains of DSG2 was unraveled in detail by X-ray diffraction analysis [16]. This molecular structure does not directly deliver data on the DSG2 mutants but provides further structural data on the localization of ARVC mutations. Interestingly, five different N-glycosylation sites and three O-mannosylation sites were identified in the extracellular part of DSG2. The amino acids carrying these PTMs are highly conserved between different vertebrate species suggesting the functional impact of these PTMs (Fig. S3, Supplements). In addition, the pattern of PTMs is also similar in different members of the desmoglein family supporting their biological impact [16]. Glycosylation is relevant in many biological processes including cell adhesion, molecular trafficking and signal transduction [27]. Remarkably, one of the human ARVC mutations (p.N182S) is affecting the second N-glycosylation site of DSG2 [28]. However, this mutation was also identified in unaffected controls (minor allele frequency: 0.0000577; http://gnomad.broadinstitute.org/variant/18-29102067-A-G, June 2018, [29]). Although the recombinantly expressed mutants do not directly affect the N-glycosylation consensus sites in DSG2-ECDs, our *in vitro* analysis reveals remarkably differential glycosylation patterns, which were not predicted from the *in silico* analysis.

Our analysis showed that the total number of glycosylation sites was not changed between WT and mutant DSG2-ECDs, whereas composition and size of the sugar structures were different. We also did not find evidence for an O-glycosylation of the mucin type in the WT and mutant DSG2-ECDs, which is in good agreement with the data from Harrison et al. 2016 [16].

The recombinantly expressed human ECDs of the ARVC associated DSG2 mutants p.D154E and p.K294E had significantly larger apparent molecular masses in comparison to the WT. After enzymatic N-deglycosylation with PNGase F, the apparent molecular masses of all but the mutation p.K294E were not different from the WT. Treatment with tunicamycin revealed that the N-glycosylation of the DSG2-ECDs can be blocked. After digestion with PNGase F, glycosylation was below the detection level of Emerald green labelling suggesting an almost complete deglycosylation of p.K294E. The mass difference of the deglycosylated DSG2-ECD p.K294E was about 4 kDa suggesting that a non-glycosylation PTM is present in this mutant. Over 200 different types of PTMs have been identified so far [30]. We excluded for this mutant also an ubiquitination (Fig. S2, Supplements). We finally could not identify which PTM was present in the mutant p.K294E, which might be part of future studies.

We also analyzed the sugar composition of the DSG2-ECDs by lectin blots. We found that lectin binding was different from the WT in the mutants p.K294E and p.V392I, when SNA was used. However, lectin binding cannot determine the size of the sugar side chains. Since we did not find a differential lectin binding of p.D154E, but a larger molecular mass, we suggest that the mass difference is caused due to the size of the sugar side chains.

N-glycosylation site inhibition revealed a larger N-glycosylation at position p.N182 for DSG2-ECD p.D154E. Using atomic force spectroscopy we have recently demonstrated that the ARVC associated DSG2 mutant p.D154E changes the kinetics of the homophilic DSG2 dimerization [15]. The sugar residues at p.N182 are localized in the second extracellular cadherin domain in close proximity to the Ca^{2+} coordination site (compare Fig. 1). This site is important for the Ca^{2+} dependent *trans*-interaction of DSG2 molecules with opposing cadherin molecules of neighboring cells [17,31]. Altered N-glycosylation may

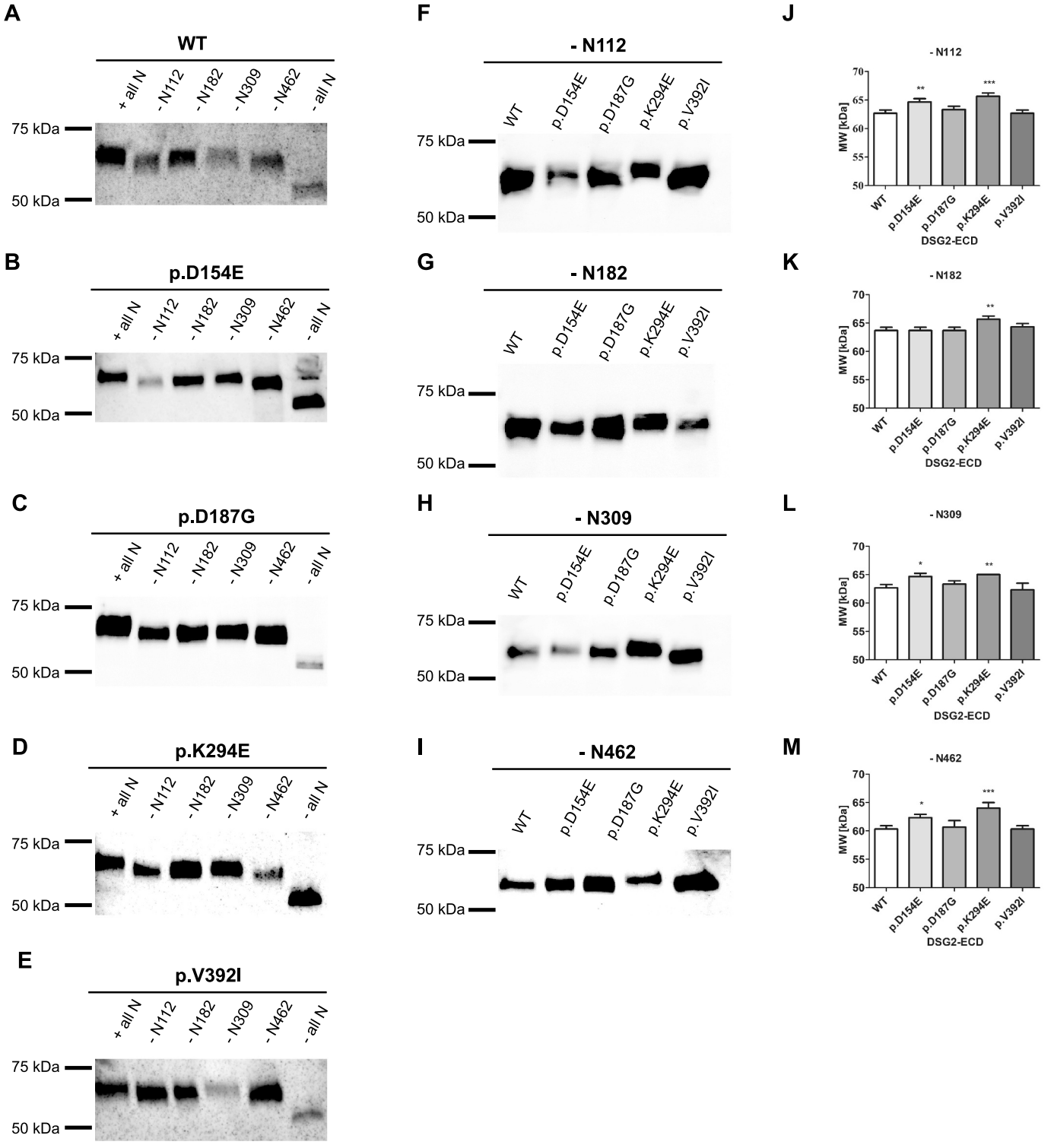

Fig. 4. DSG2-ECD p.D154E is differentially glycosylated at p.N182.
(A–E) N-glycosylation deficient DSG2-ECD WT and mutants without (−) N-glycosylation at N112, N182, N309 or N462 show a consistently and significantly decreased apparent molecular mass compared to their completely glycosylated controls (+all N) confirming N-glycosylation at all four positions in DSG2-ECD WT as well as in all ARVC associated mutants. (F-M) N-glycosylation deficient DSG2-ECD mutants p.D154E and p.K294E without (−) N-glycosylation at N112, N309 or N462 display significantly different molecular masses compared to the WT. The mutant DSG2-ECD p.D154E without N-glycosylation at p.N182 had no significantly different mass in comparison to the WT (G, K), suggesting a larger N-glycosylation at this position. N-glycosylation deficient DSG2-ECD p.K294E showed a significantly diverse apparent molecular mass suggesting another PTM.

disturb the molecular architecture contributing to nano-mechanical binding defects.

The recently described molecular structure of the extracellular domains of DSG2, revealed three O-mannosylation sites (p.T480, p.T482 and p.T484) in the fourth extracellular domain of DSG2 [16]. O-mannosylations are rare sugar modifications, which have been recently

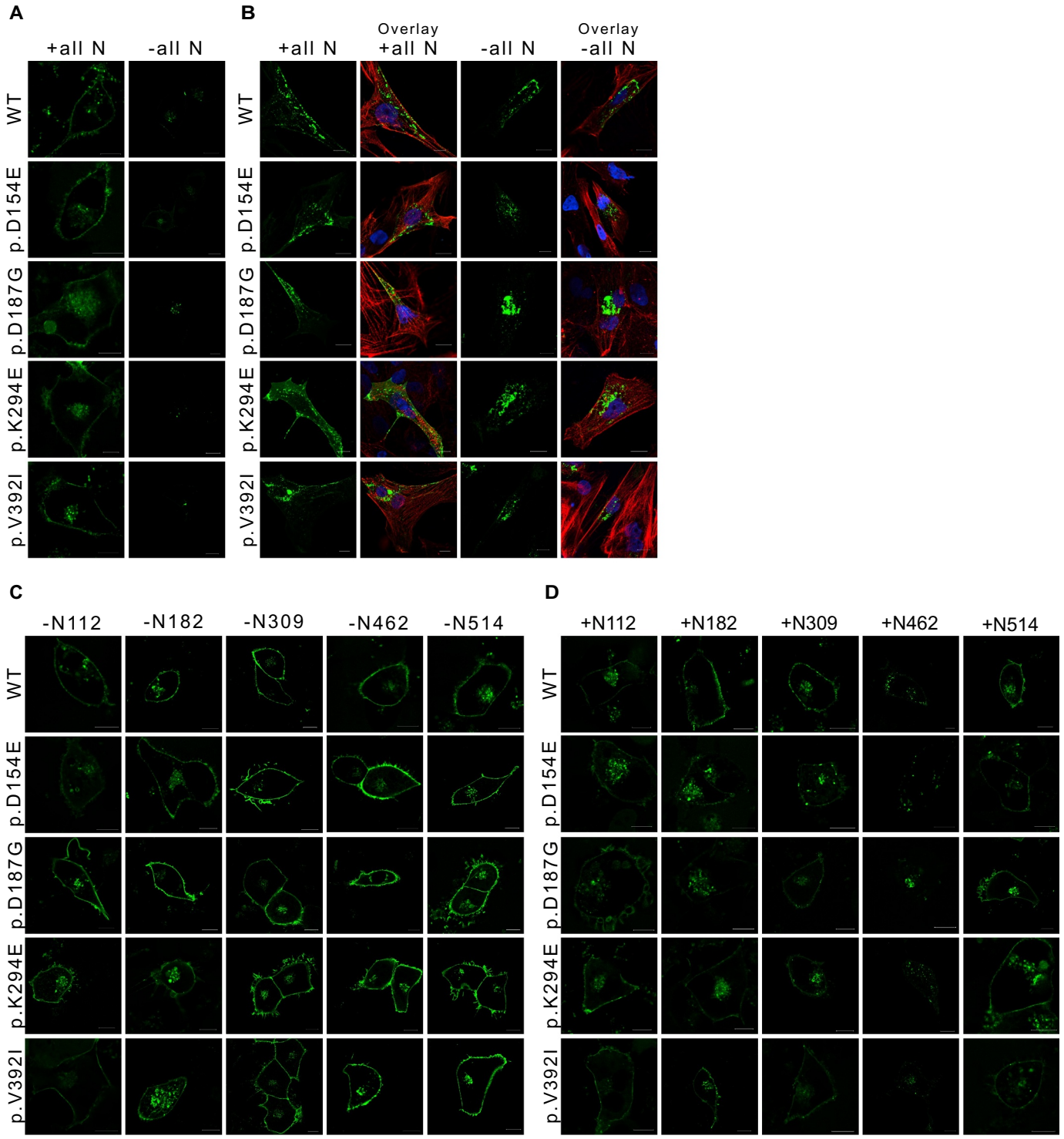

Fig. 5. Mutation of multiple N-glycosylation sites blocks the efficient transport of DSG2 to the plasma membrane.
Representative fluorescence images of transfected living HT1080 cells and fixed hiPSC derived cardiomyocytes were shown. (A-B) In contrast to completely glycosylated (+all N) WT and mutant DSG2, N-glycosylation deficient DSG2 WT and mutants without any N-glycosylations (−all N) were primarily localized in intracellular structures in HT1080 cells (A) and hiPSC derived cardiomyocytes (B). (C) Similar to completely glycosylated WT and mutant DSG2, N-glycosylation deficient DSG2 WT and mutants without (−) N-glycosylation at N112, N182, N309, N462 or N514 were localized at the plasma membrane in HT1080 cells. (D) N-glycosylation deficient DSG2 WT and mutants with single (+) N-glycosylation at N112, N182, N309, N462 or N514 were localized at the plasma membrane in HT1080 cells. DSG2 is shown in green, nuclear staining (DAPI) in blue and anti α-actinin staining as cardiomyocyte marker in red. Scale bars represent 10 μm.

identified in several members of the cadherin family [32–34]. In our study, no carbohydrates were detectable after enzymatic digestion using PNGase F suggesting that O-mannosylation was not present or below the limit of detection of Pro-Q® Emerald 300 glycoprotein staining, respectively. Similar effects were observed by lectin binding analysis. After PNGase F treatment of DSG2-ECD WT and mutants no lectin binding was observed at all, suggesting that potential O-mannosylated glycans would probably not be further elongated. These

Table 1
Dispase based cell dissociation assay.

DSG2 genotype	Number of fragments (means ± SD)	ANOVA[§]
WT	17.5 ± 6.3[$]	–
p.D154E	8.7 ± 4.3[$]	***
p.D187G	8.9 ± 3.8	***
p.K294E	14.8 ± 5.6	ns
p.V392I	18.04 ± 12.32[$]	ns

[§] ANOVA with Dunnett's Multiple Comparison Test.
*** $P < 0.001$ for pairs WT/p.D154E and WT/p.D187G.
[$] Data given for comparison and previously published in [15].

observations are consistent with findings from other groups indicating that O-mannosylated glycans of cadherins are not further elongated [32,33].

Up to now, no *knock-in* mice of human cardiomyopathy associated DSG2 mutations have been reported and only little functional data on the mutant proteins are available. We previously found that the mutants DSG2 p.R46Q, p.D154E and p.V392I revealed *in vitro* aberrant binding properties when compared to the WT [15,19]. Although we used different assays to characterize the binding properties we found conclusively that the protein-protein binding of these mutants appeared to be more stable than for the WT form. In this study, we used a dispase based assay and found that p.D187G also leads to a stronger interaction in the cell based test system, whereas the mutation p.K294E did not show differences to the controls. This is remarkable since this mutant revealed a differential PTM. We also analyzed if the transport of DSG2 might be affected by the mutation. We tested single glycosylated mutants or mutants lacking only one N-glycosylation site. Surprisingly, we found that even one glycosylated N-residue is sufficient to direct DSG2 to the cell surface. We used in our study HT1080 cells, which were previously used as model systems for the investigation of desmosomal proteins [17,35,36]. We also tested hiPSC derived cardiomyocytes which confirmed the findings of the corresponding experiment with HT1080 cells. Although we did not evaluate DGS2-surface expression in a quantitative manner, the data may provide evidence that both cell types handle DSG2 expression in a comparable way.

Changes in the glycosylation pattern were recently found in a model of rat hypertrophic cardiomyopathy [37,38]. Thus, differential glycosylation patterns in cardiac disease might also be of more general impact. However, to the best of our knowledge the aberrant glycosylation patterns of proteins were not shown before in arrhythmogenic right ventricular cardiomyopathies.

Thus, here we provide evidence *in vitro* insights into behavior of mutant DSG2 can unfortunately not be directly translated into genetic counseling. The pathogenic interpretation of *DSG2* missense mutations remains therefore challenging and is more complex than previously anticipated.

5. Conclusions

In summary, we present here data, which indicate that ARVC associated *DSG2* mutations affect the glycosylation stage of the protein although these mutations do not directly change the N-glycosylation consensus sequences. Our analyses showed that the total number of glycosylation sites was not changed in the mutant DSG2-ECDs, whereas the composition and size of the sugar structures are different. Surprisingly, we found that even one glycosylated N-residue is

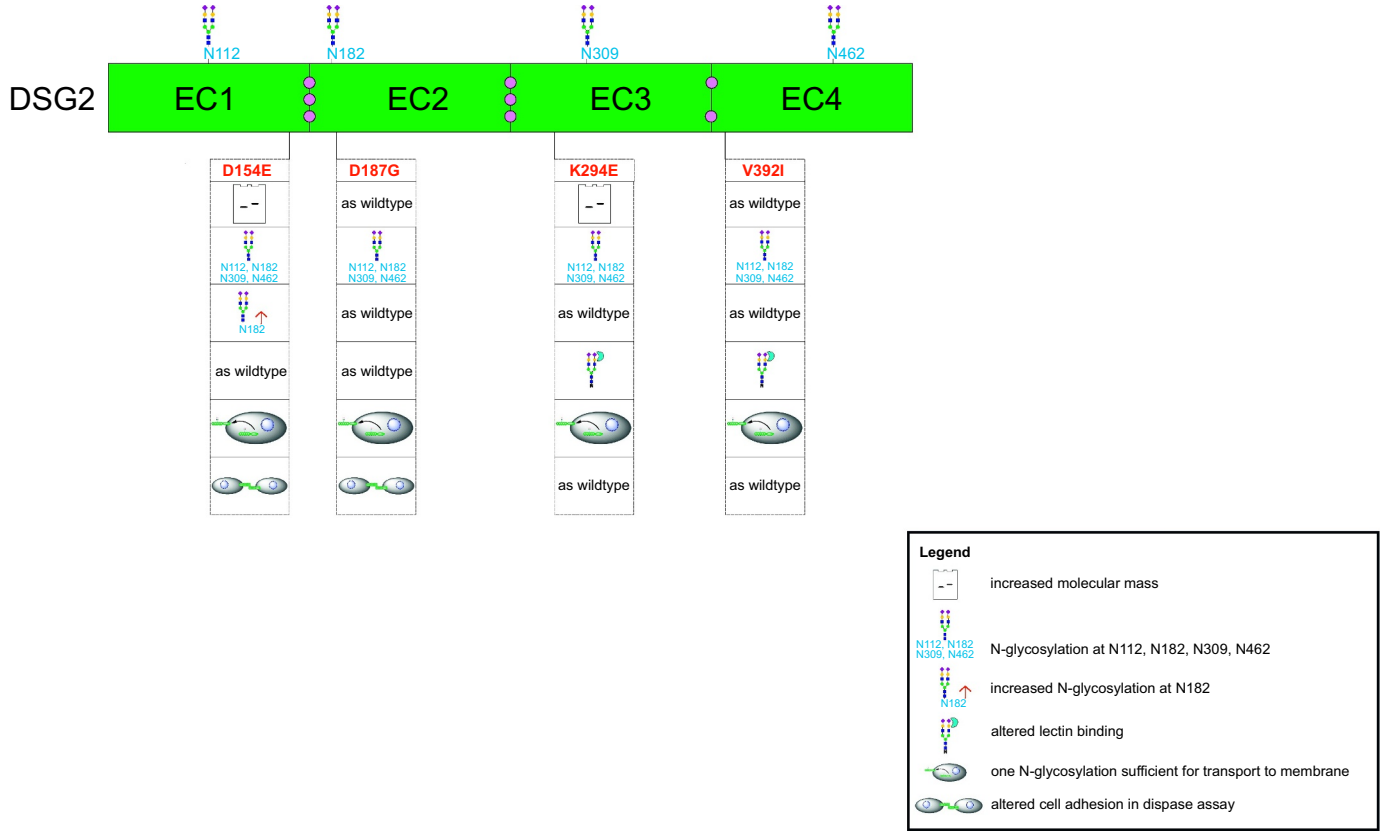

Fig. 6. Overview on the main results of the manuscript.
Schematic graphic of the extracellular cadherin domains (EC1-4) of DSG2 with N-glycosylations (N112, N182, N309, N462) and complexed Ca^{2+}-ions (purple). For the ARVC-associated mutations analyzed in the study (D154E, D187G, K294E, V392I) the experimental results are illustrated by pictograms and deviations from wildtype conditions are displayed (for further explanation see legend). For generation of the scheme Adobe Illustrator CC (v.22.1) and ChemDraw Professional (v. 16.0.1.4, Perkin Elmer) was used.

sufficient to direct DSG2 to the cell surface. Our study reveals complex molecular interactions between *DSG2* mutations and N-glycosylations of DSG2, which may contribute to the molecular understanding of the patho-mechanisms associated with ARVC.

Acknowledgements

We would like to thank Daniela Baurichter for support with confocal microscopy. The authors would like to thank the Genome Aggregation Database (gnomAD) and the groups that provided exome and genome variant data to this resource [29]. A full list of contributing groups can be found at http://gnomad.broadinstitute.org/about. In addition, we thank Dr. Dr. Tomo Saric (University of Cologen, Germany) for providing the hiPSC UKKi011-A.

Funding

HM and DA are kindly supported by a grant of the German Research Foundation (DFG, MI-1146/2-1 & DA-370/6-1) and the Erich and Hanna Klessmann Foundation (Gütersloh, Germany). AB, JG and HM are grateful for financial support by the German Society of Heart Research and also by the University of Bielefeld (Forschungsfonds OWL). AGR received a research grant of the Medical Faculty of the Ruhr-University of Bochum (FoRUM).

Appendix A. Supplementary data

Supplementary data to this article can be found online at https://doi.org/10.1016/j.yjmcc.2019.03.014.

References

[1] D. Corrado, C. Basso, G. Thiene, W.J. McKenna, M.J. Davies, F. Fontaliran, A. Nava, F. Silvestri, C. Blomstrom-Lundqvist, E.K. Wlodarska, G. Fontaine, F. Camerini, Spectrum of clinicopathologic manifestations of arrhythmogenic right ventricular cardiomyopathy/dysplasia: a multicenter study, J. Am. Coll. Cardiol. 30 (6) (1997) 1512–1520.

[2] D. Corrado, F. Migliore, C. Basso, G. Thiene, Exercise and the risk of sudden cardiac death, Herz 31 (6) (2006) 553–558.

[3] C. Basso, G. Thiene, Adipositas cordis, fatty infiltration of the right ventricle, and arrhythmogenic right ventricular cardiomyopathy. Just a matter of fat? Cardiovasc. Pathol. 14 (1) (2005) 37–41.

[4] B.J. Maron, J.A. Towbin, G. Thiene, C. Antzelevitch, D. Corrado, D. Arnett, A.J. Moss, C.E. Seidman, J.B. Young, A. American Heart, H.F, Council on Clinical Cardiology, C, Transplantation, C, Quality of, R. Outcomes, G. Functional, G. Translational Biology Interdisciplinary Working, E, Council on, Prevention, Contemporary definitions and classification of the cardiomyopathies: an American Heart Association Scientific Statement from the Council on Clinical Cardiology, Heart Failure and Transplantation Committee; Quality of Care and Outcomes Research and Functional Genomics and Translational Biology Interdisciplinary Working Groups; and Council on Epidemiology and Prevention, Circulation 113 (14) (2006) 1807–1816.

[5] P. Syrris, D. Ward, A. Evans, A. Asimaki, E. Gandjbakhch, S. Sen-Chowdhry, W.J. McKenna, Arrhythmogenic right ventricular dysplasia/cardiomyopathy associated with mutations in the desmosomal gene desmocollin-2, Am. J. Hum. Genet. 79 (5) (2006) 978–984.

[6] A. Heuser, E.R. Plovie, P.T. Ellinor, K.S. Grossmann, J.T. Shin, T. Wichter, C.T. Basson, B.B. Lerman, S. Sasse-Klaassen, L. Thierfelder, C.A. MacRae, B. Gerull, Mutant desmocollin-2 causes arrhythmogenic right ventricular cardiomyopathy, Am. J. Hum. Genet. 79 (6) (2006) 1081–1088.

[7] A. Rampazzo, A. Nava, S. Malacrida, G. Beffagna, B. Bauce, V. Rossi, R. Zimbello, B. Simionati, C. Basso, G. Thiene, J.A. Towbin, G.A. Danieli, Mutation in human desmoplakin domain binding to plakoglobin causes a dominant form of arrhythmogenic right ventricular cardiomyopathy, Am. J. Hum. Genet. 71 (5) (2002) 1200–1206.

[8] G. McKoy, N. Protonotarios, A. Crosby, A. Tsatsopoulou, A. Anastasakis, A. Coonar, M. Norman, C. Baboonian, S. Jeffery, W.J. McKenna, Identification of a deletion in plakoglobin in arrhythmogenic right ventricular cardiomyopathy with palmoplantar keratoderma and woolly hair (Naxos disease), Lancet 355 (9221) (2000) 2119–2124.

[9] B. Gerull, A. Heuser, T. Wichter, M. Paul, C.T. Basson, D.A. McDermott, B.B. Lerman, S.M. Markowitz, P.T. Ellinor, C.A. MacRae, S. Peters, K.S. Grossmann, J. Drenckhahn, B. Michely, S. Sasse-Klaassen, W. Birchmeier, R. Dietz, G. Breithardt, E. Schulze-Bahr, L. Thierfelder, Mutations in the desmosomal protein plakophilin-2 are common in arrhythmogenic right ventricular cardiomyopathy, Nat. Genet. 36 (11) (2004) 1162–1164.

[10] B. Klauke, S. Kossmann, A. Gaertner, K. Brand, I. Stork, A. Brodehl, M. Dieding, V. Walhorn, D. Anselmetti, D. Gerdes, B. Bohms, U. Schulz, E. Zu Knyphausen, M. Vorgerd, J. Gummert, H. Milting, De novo desmin-mutation N116S is associated with arrhythmogenic right ventricular cardiomyopathy, Hum. Mol. Genet. 19 (23) (2010) 4595–4607.

[11] P. Syrris, D. Ward, A. Asimaki, A. Evans, S. Sen-Chowdhry, S.E. Hughes, W.J. McKenna, Desmoglein-2 mutations in arrhythmogenic right ventricular cardiomyopathy: a genotype-phenotype characterization of familial disease, Eur. Heart J. 28 (5) (2007) 581–588.

[12] M.M. Awad, D. Dalal, E. Cho, N. Amat-Alarcon, C. James, C. Tichnell, A. Tucker, S.D. Russell, D.A. Bluemke, H.C. Dietz, H. Calkins, D.P. Judge, DSG2 mutations contribute to arrhythmogenic right ventricular dysplasia/cardiomyopathy, Am. J. Hum. Genet. 79 (1) (2006) 136–142.

[13] K. Pilichou, A. Nava, C. Basso, G. Beffagna, B. Bauce, A. Lorenzon, G. Frigo, A. Vettori, M. Valente, J. Towbin, G. Thiene, G.A. Danieli, A. Rampazzo, Mutations in desmoglein-2 gene are associated with arrhythmogenic right ventricular cardiomyopathy, Circulation 113 (9) (2006) 1171–1179.

[14] H.A. Thomason, A. Scothern, S. McHarg, D.R. Garrod, Desmosomes: adhesive strength and signalling in health and disease, Biochem. J. 429 (3) (2010) 419–433.

[15] M. Dieding, J.D. Debus, R. Kerkhoff, A. Gaertner-Rommel, V. Walhorn, H. Milting, D. Anselmetti, Arrhythmogenic cardiomyopathy related DSG2 mutations affect desmosomal cadherin binding kinetics, Sci. Rep. 7 (1) (2017) 13791.

[16] O.J. Harrison, J. Brasch, G. Lasso, P.S. Katsamba, G. Ahlsen, B. Honig, L. Shapiro, Structural basis of adhesive binding by desmocollins and desmogleins, Proc. Natl. Acad. Sci. U. S. A. 113 (26) (2016) 7160–7165.

[17] N.A. Chitaev, S.M. Troyanovsky, Direct Ca2 + −dependent heterophilic interaction between desmosomal cadherins, desmoglein and desmocollin, contributes to cell-cell adhesion, J. Cell Biol. 138 (1) (1997) 193–201.

[18] S.E. Syed, B. Trinnaman, S. Martin, S. Major, J. Hutchinson, A.I. Magee, Molecular interactions between desmosomal cadherins, Biochem. J. 362 (Pt 2) (2002) 317–327.

[19] A. Gaertner, B. Klauke, I. Stork, K. Niehaus, G. Niemann, J. Gummert, H. Milting, In vitro functional analyses of arrhythmogenic right ventricular cardiomyopathy-associated desmoglein-2-missense variations, PLoS One 7 (10) (2012) e47097.

[20] T. Xu, Z. Yang, M. Vatta, A. Rampazzo, G. Beffagna, K. Pilichou, S.E. Scherer, J. Saffitz, J. Kravitz, W. Zareba, G.A. Danieli, A. Lorenzon, A. Nava, B. Bauce, G. Thiene, C. Basso, H. Calkins, K. Gear, F. Marcus, J.A. Towbin, I. Multidisciplinary Study of Right Ventricular Dysplasia, Compound and digenic heterozygosity contributes to arrhythmogenic right ventricular cardiomyopathy, J. Am. Coll. Cardiol. 55 (6) (2010) 587–597.

[21] I.J. Goldstein, C.E. Hayes, The lectins: carbohydrate-binding proteins of plants and animals, Adv. Carbohydr. Chem. Biochem. 35 (1978) 127–340.

[22] P.D. Stenson, M. Mort, E.V. Ball, K. Evans, M. Hayden, S. Heywood, M. Hussain, A.D. Phillips, D.N. Cooper, The Human Gene Mutation Database: towards a comprehensive repository of inherited mutation data for medical research, genetic diagnosis and next-generation sequencing studies, Hum. Genet. 136 (6) (2017) 665–677.

[23] P.A. van der Zwaag, J.D. Jongbloed, M.P. van den Berg, J.J. van der Smagt, R. Jongbloed, H. Bikker, R.M. Hofstra, J.P. van Tintelen, A genetic variants database for arrhythmogenic right ventricular dysplasia/cardiomyopathy, Hum. Mutat. 30 (9) (2009) 1278–1283.

[24] L. Eshkind, Q. Tian, A. Schmidt, W.W. Franke, R. Windoffer, R.E. Leube, Loss of desmoglein 2 suggests essential functions for early embryonic development and proliferation of embryonal stem cells, Eur. J. Cell Biol. 81 (11) (2002) 592–598.

[25] S. Kant, B. Holthofer, T.M. Magin, C.A. Krusche, R.E. Leube, Desmoglein 2-dependent Arrhythmogenic cardiomyopathy is caused by a loss of adhesive function, Circ. Cardiovasc. Genet. 8 (4) (2015) 553–563.

[26] C.A. Krusche, B. Holthofer, V. Hofe, A.M. van de Sandt, L. Eshkind, E. Bockamp, M.W. Merx, S. Kant, R. Windoffer, R.E. Leube, Desmoglein 2 mutant mice develop cardiac fibrosis and dilation, Basic Res. Cardiol. 106 (4) (2011) 617–633.

[27] K. Ohtsubo, J.D. Marth, Glycosylation in cellular mechanisms of health and disease, Cell 126 (5) (2006) 855–867.

[28] T.J. Pugh, M.A. Kelly, S. Gowrisankar, E. Hynes, M.A. Seidman, S.M. Baxter, M. Bowser, B. Harrison, D. Aaron, L.M. Mahanta, N.K. Lakdawala, G. McDermott, E.T. White, H.L. Rehm, M. Lebo, B.H. Funke, The landscape of genetic variation in dilated cardiomyopathy as surveyed by clinical DNA sequencing, Genet. Med. 16 (8) (2014) 601–608.

[29] M. Lek, K.J. Karczewski, E.V. Minikel, K.E. Samocha, E. Banks, T. Fennell, A.H. O'Donnell-Luria, J.S. Ware, A.J. Hill, B.B. Cummings, T. Tukiainen, D.P. Birnbaum, J.A. Kosmicki, L.E. Duncan, K. Estrada, F. Zhao, J. Zou, E. Pierce-Hoffman, J. Berghout, D.N. Cooper, N. Deflaux, M. DePristo, R. Do, J. Flannick, M. Fromer, L. Gauthier, J. Goldstein, N. Gupta, D. Howrigan, A. Kiezun, M.I. Kurki, A.L. Moonshine, P. Natarajan, L. Orozco, G.M. Peloso, R. Poplin, M.A. Rivas, V. Ruano-Rubio, S.A. Rose, D.M. Ruderfer, K. Shakir, P.D. Stenson, C. Stevens, B.P. Thomas, G. Tiao, M.T. Tusie-Luna, B. Weisburd, H.H. Won, D. Yu, D.M. Altshuler, D. Ardissino, M. Boehnke, J. Danesh, S. Donnelly, R. Elosua, J.C. Florez, S.B. Gabriel, G. Getz, S.J. Glatt, C.M. Hultman, S. Kathiresan, M. Laakso, S. McCarroll, M.I. McCarthy, D. McGovern, R. McPherson, B.M. Neale, A. Palotie, S.M. Purcell, D. Saleheen, J.M. Scharf, P. Sklar, P.F. Sullivan, J. Tuomilehto, M.T. Tsuang, H.C. Watkins, J.G. Wilson, M.J. Daly, D.G. MacArthur, C. Exome Aggregation, Analysis of protein-coding genetic variation in 60,706 humans, Nature 536 (7616) (2016) 285–291.

[30] S. Prabakaran, G. Lippens, H. Steen, J. Gunawardena, Post-translational modification: nature's escape from genetic imprisonment and the basis for dynamic information encoding, Wiley Interdiscipl. Rev. Syst. Biol. Med. 4 (6) (2012) 565–583.

[31] A. Schlipp, C. Schinner, V. Spindler, F. Vielmuth, K. Gehmlich, P. Syrris,

W.J. McKenna, A. Dendorfer, E. Hartlieb, J. Waschke, Desmoglein-2 interaction is crucial for cardiomyocyte cohesion and function, Cardiovasc. Res. 104 (2) (2014) 245–257.
[32] I.S.B. Larsen, Y. Narimatsu, H.J. Joshi, Z. Yang, O.J. Harrison, J. Brasch, L. Shapiro, B. Honig, S.Y. Vakhrushev, H. Clausen, A. Halim, Mammalian O-mannosylation of cadherins and plexins is independent of protein O-mannosyltransferases 1 and 2, J. Biol. Chem. 292 (27) (2017) 11586–11598.
[33] I.S.B. Larsen, Y. Narimatsu, H.J. Joshi, L. Siukstaite, O.J. Harrison, J. Brasch, K.M. Goodman, L. Hansen, L. Shapiro, B. Honig, S.Y. Vakhrushev, H. Clausen, A. Halim, Discovery of an O-mannosylation pathway selectively serving cadherins and protocadherins, Proc. Natl. Acad. Sci. U. S. A. 114 (42) (2017) 11163–11168.
[34] M. Lommel, P.R. Winterhalter, T. Willer, M. Dahlhoff, M.R. Schneider, M.F. Bartels, I. Renner-Muller, T. Ruppert, E. Wolf, S. Strahl, Protein O-mannosylation is crucial for E-cadherin-mediated cell adhesion, Proc. Natl. Acad. Sci. U. S. A. 110 (52) (2013) 21024–21029.
[35] E.A. Bornslaeger, L.M. Godsel, C.M. Corcoran, J.K. Park, M. Hatzfeld, A.P. Kowalczyk, K.J. Green, Plakophilin 1 interferes with plakoglobin binding to desmoplakin, yet together with plakoglobin promotes clustering of desmosomal plaque complexes at cell-cell borders, J. Cell Sci. 114 (Pt 4) (2001) 727–738.
[36] J. Koeser, S.M. Troyanovsky, C. Grund, W.W. Franke, De novo formation of desmosomes in cultured cells upon transfection of genes encoding specific desmosomal components, Exp. Cell Res. 285 (1) (2003) 114–130.
[37] C. Nagai-Okatani, N. Minamino, Aberrant glycosylation in the left ventricle and plasma of rats with cardiac hypertrophy and heart failure, PLoS One 11 (6) (2016) e0150210.
[38] I. Gudelj, G. Lauc, Protein N-glycosylation in cardiovascular diseases and related risk factors, Curr. Cardiovasc. Risk Rep. 12 (6) (2018).